On the Friction Behavior of SiO₂ Tip Sliding on Au (111) Surface: How an Amorphous SiO₂ Tip Produces Regular Stick-Slip Friction and Friction Duality?

Rong-Guang Xu^a, Gunan Zhang^a, Yuan Xiang^a, and Yongsheng Leng^{a*}

^a Department of Mechanical and Aerospace Engineering, The George Washington University, 800 22nd Street N.W., Washington, DC 20052, United States

*Email: leng@gwu.edu

Abstract

Friction behaviors of an amorphous SiO₂ tip sliding on an Au (111) surface in atomic force microscopy (AFM) are investigated through molecular dynamics (MD) simulations. We observed a regime of extremely low, close-to-zero friction at low normal loads with clear stick-slip friction signals. The friction is almost independent of the applied normal load below a threshold value. However, above this loading threshold, friction can remain low or increase sharply. Such an unexpected friction duality is attributed to the high probability of defect formation at the sliding interface that can induce plowing friction in a high-friction state. The energy difference between the low-friction state and the high-friction state is surprisingly low, which is comparable to kT (~ 25 meV) at room temperature. These findings are consistent with previous AFM friction measurements using silicon AFM tips. Further MD simulations show that one can always use an amorphous SiO₂ tip to image the crystalline surface with regular stick-slip friction signals. This is largely due to the fact that there are always a small fraction of contacting Si and O atoms at the sliding interface that are sitting on the relatively stable, close-to-hollow sites of the crystalline Au (111) surface during the stick stage, thus they are capable of sampling local energy minima. We anticipate that regular stick-slip friction could be achieved even in the intermediate loading range, so long as the low-friction state is maintained when friction duality occurs.

1

INTRODUCTION

There are a variety of technological applications and scientific curiosities involving friction between two sliding surfaces ¹⁻⁵. Understanding the friction behavior of a single asperity contact at nanometer scale is crucial to minimizing friction losses and wear, and enhancing the reliability of future micro and nanoscale devices ⁶.

Since the invention of atomic force microscope (AFM)⁷ and its application in fundamental studies of atomic-scale friction⁸, friction measurements by an AFM tip frequently showed regular stick-slip friction signals with atomic-scale resolutions. The microstructure of the tip apex could be a polycrystalline metal apex (for instance, the AFM tip made from the thermally evaporated metal coating on a silicon cantilever⁹), or an amorphous nonmetallic material such as a silicon oxide (SiO₂) ¹⁰⁻¹¹. In our previous paper¹², molecular dynamics (MD) simulations of a polycrystalline Pt tip (R = 10 nm in radius) sliding on an Au (111) surface revealed how the geometry of the polycrystalline tip take effect on the friction behavior at the contact interface. We found that if the apex of an AFM tip has multiple neighboring grains near the edge of contact, plastic deformations near this contact edge likely happen, leading to irregular stick—slip high friction upon sliding. However, when the apex of the Pt tip adopts a single crystalline protrusion without any neighboring grains involved in the metal contact, a clear stick—slip friction signal with single atomic slips could be achieved.

In this work, we shift our focus on the friction simulations of an amorphous SiO₂ tip sliding on an Au (111) substrate. Compared with the sliding friction of a Pt tip on an Au (111) surface¹², the amorphous SiO₂ tip in contact with an Au (111) surface in sliding friction is a more challenging topic because the contact geometry and chemistry at the tip apex are largely unknown in an AFM friction experiment. Usually, a silicon AFM tip has an amorphous oxide film of about 2-3 nm thick at the tip apex¹³⁻¹⁴. The chemical nature of this oxide film (SiOx) is very complex. It was generally believed that after heat treatment in vacuum, there are very few –OH groups on the oxide surface¹⁴. This will be the basis to build AFM silicon tip models. The detailed atomic structure of SiO_x network has a direct impact on the quantitative measurement of mechanical properties, conductivity, friction force, and wear resistance¹³. Previous representative experimental studies for such an amorphous silicon tip sliding on an Au(111) surface are found in references ^{10-11, 15-16}.

Here, we investigate the atomic-scale friction of an amorphous SiO₂ tip sliding on an Au (111) surface by carrying out straightforward MD simulations. Our focus is to understand (1) how an

amorphous SiO₂ tip can still produce clear stick-slip friction signals; and (2) how the friction dissipation depends on the applied normal load.

Very interestingly, for the second question we find that when the normal load is below a threshold value, friction is almost independent of the applied normal load. Above this loading threshold, however, friction may remain low or increase sharply. Such an unexpected friction *duality*, although was studied previously for a very different friction system (An amorphous Sb nanoparticle sliding on a highly oriented pyrolytic graphite (HOPG) substrate)¹⁷⁻¹⁹, has not yet been properly explained.

This paper will first explore the mechanism of friction duality observed for the SiO₂/Au (111) contact. Historically, the complex relation between friction and external normal load beyond the Amontons' laws had been explored substantially in the past more than 30 years (see references 4, ²⁰). A variety of load dependence of friction at nanoscale was also discussed²¹. There is often a linear load dependence observed for non-adhesive systems, whereas sub-linear characteristics are observed for adhesive systems²². So far the load-dependent friction could be linear²³⁻²⁴, sublinear²⁰, ^{22, 25-27}, or faster than linear¹⁰. For amorphous silicon/metal contacts, Gosvami et al. ^{10, 28} observed extremely low, close-to-zero friction with a clear stick-slip behavior on clean and atomically flat metal surfaces, such as Cu (100) and Au (111) surfaces under low loads. The friction is independent of the applied normal load up to a threshold value, above which friction force and its fluctuations increase sharply due to the onset of wear, accompanied by irregular stick-slip friction and the loss of atomic periodicity. While these observations were similar to what we found in this work through MD simulations, interpretation to the observed low and high frictions was attributed to the formation of a crystalline metallic neck between the tip and the surface ²⁹⁻³¹. Under high loads, the metallic neck breaks down and the irregular stick-slip behavior is associated with the onset of wear.

Here, we provide an alternative interpretation to the SiO₂ tip/Au (111) friction through direct MD simulations. We find that high friction with irregular stick-slips is due to the generation of defects on the Au (111) surface in which only a few Au atoms are involved. This is in contrast to the formation of metallic neck between the silicon tip and the gold surface. The friction duality observed in MD simulations is uniquely related to whether or not the defect formation on the Au (111) surface. Such an explanation is also fundamentally different from the interpretation of friction duality observed for the case of an amorphous Sb nanoparticle sliding on a HOPG substrate

¹⁷⁻¹⁹, in which the ultralow friction was attributed to the superlubric behavior due to the structural mismatch between the nanoparticle and the HOPG substrate ¹⁷.

This paper is organized as follows. In Section 2 we briefly describe the method of building amorphous SiO₂ tip/Au (111) contact in an MD simulation system and the detailed MD simulation approach. Section 3 will present detailed simulation results, including friction force variations with load and the mechanism of how an amorphous SiO₂ tip sliding on an Au (111) surface can still produce regular stick-slip friction. We conclude our simulation studies in Section 4.

MATERIALS AND METHODS

The MD simulation setup is shown in Fig. 1. The Au (111) substrate has a dimension of 20 nm × 16 nm × 1.9 nm (length × width × thickness) with a crystallographic orientation of [111] in the z-direction. The x and y axes are along the $[1\overline{10}]$ and $[11\overline{2}]$ directions, respectively. Periodic boundary conditions are applied in both x- and y-directions. The gold substrate is relaxed at 300 K with the bottom two layers fixed. The embedded atom method (EAM)³²⁻³³ with Voter's modifications³⁴ is employed for Au interatomic interactions. Two different SiO₂ tips are constructed in this study: (i) a small tip in a truncated cone geometry with a height of 3 nm. The top and bottom surfaces each has a diameter of 3 nm and 2 nm, respectively; and (ii) a large tip with the same height (3 nm) in a cone geometry but the diameters of both top and bottom surfaces are doubled (6 nm and 4 nm, respectively). Amorphous SiO₂ tips are obtained by quenching a bulk SiO₂ and then cutting the block to the desired tip geometry, followed by a 4 ns-MD relaxation for the tip-Au (111) contact at zero normal load to reach equilibration. The total numbers of Si and O atoms in the small and large SiO₂ tips are 896 and 3268, respectively. The interatomic interactions within the SiO₂ tip are described by the Tersoff potentials³⁵. The topmost atoms in the tip are treated as a rigid body which is subjected to external normal load by the connected lateral harmonic springs. Sliding motion is along the x-direction by moving the support at a constant velocity as shown in Fig. 1. The sliding speed is set to v = 1 m/s throughout simulations. The lateral spring constant is set to $k_x = 5.36$ N/m, while the stiffness of the spring along the y-direction is much higher ($k_v = 300 \text{ N/m}$), making the motion of the tip along the axial direction of the cantilever largely constrained.

Interactions between the SiO₂ tip and the Au substrate are modeled by the Lennard-Jones (LJ) potential, as has been validated in previous simulation studies¹¹ (for Si-Au: ε =0.0047 eV and σ =3.38 Å; and for O-Au: ε =0.0033 eV and σ =3.04 Å). The LAMMPS package ³⁶⁻³⁷ is used throughout this simulation study. The MD time step is set to 1.0 fs. The temperature of the system is controlled by the Nosé–Hoover thermostat³⁸⁻³⁹ at 300K.

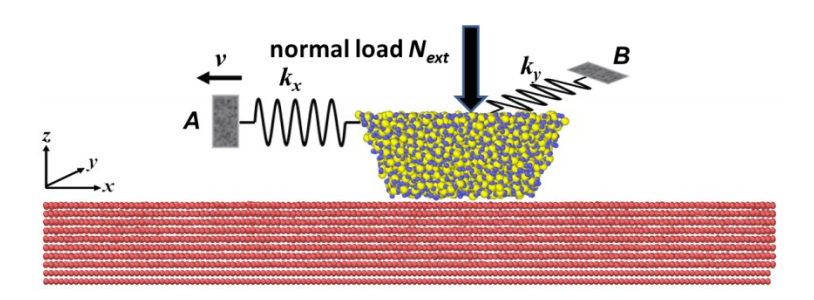


Figure 1. The MD simulation setup. Au, Si and O atoms are in red, blue and yellow, respectively. The color scheme is consistent throughout this work.

In MD friction simulations, external normal load N_{ext} (**Fig. 1**) is directly applied on the topmost atoms of the SiO₂ tip. Upon N_{ext} is applied on the tip, an equilibrium MD run of 0.5 ns is further carried out to equilibrate the system, followed by a full forward-backward friction loop simulation over a 5 nm-sliding distance under the same load, which takes a total of 10 ns simulation time. Mean friction forces are then calculated as the areas inside the friction loops divided by the sliding distance. A total of *five* independent MD runs are carried out for each load. The error bar under each normal load is determined as the standard deviation during the averaging.

SIMULATION RESULTS AND DISCUSSIONS

A. Friction versus normal load

Figure 2a shows variations of the mean friction force versus external normal load for both small and large SiO_2 tips. Typical friction loops under $N_{ext} = 12$ nN for both tips are shown in Fig. 3a and 3b, respectively, which present clear atomic stick-slip friction. Essentially, under low normal loads up to 12nN, friction is almost negligible. However, as the normal load is increased continuously, high-friction state for the small SiO_2 tip begins to emerge, in which stick-slip friction

exhibits irregular single and double slips, as shown in **Fig. 3c** for $N_{ext} = 18$ nN. Such a friction transition on the Au (111) surface is strikingly similar to previous experimental measurements by Gosvami et al.^{10, 28}. We find that at $N_{ext} = 18$ nN, the small SiO₂ tip simply displaces a single gold atom away from the gold substrate, creating a vacancy defect and an ad-atom on the Au (111) surface (**Fig. 3d**). In general, more interfacial defects will be created under higher normal loads. We find that only one surface defect is found in the loading range from 14 - 27 nN, but more than three surface defects are seen when the normal load is increased to 30 - 33 nN, and more than six are seen when the normal load $N_{ext} > 36$ nN. This surface-defect-induced high friction is in contrast to the interpretation of metallic necking formation between the SiO₂ tip and the Au substrate ²⁸. The latter attributes the overall friction property of the SiO₂/Au (111) contact to the friction behavior of the metal necking junction, which was presumably created due to the diffusion of large numbers of gold atoms around the SiO₂/Au (111) contact ¹⁰.

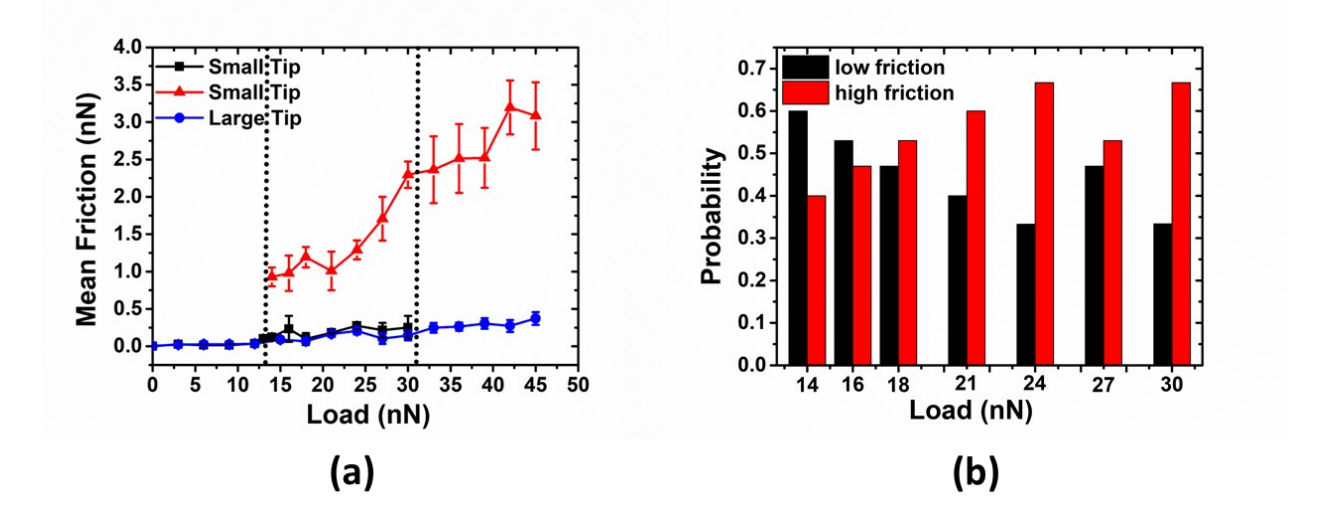


Figure 2. (a) Mean friction forces as a function of applied normal load for two different tips. For the small SiO_2 tip, friction duality of low- and high-friction states is observed in the intermediate range of the load between 14 - 33 nN. For the large SiO_2 tip, only low-friction state is observed in the whole range of normal load investigated without any surface defects created. (b) The probability of the occurrence of low- and high-friction states under intermediate loading range for the small SiO_2 tip.

As shown in **Fig. 2a**, an outstanding friction *duality* occurs for the small SiO_2 tip when the normal load N_{ext} is in the range of 14 - 33 nN. In this intermediate loading range, there are two possible friction states, namely, the low- and high-friction states. The latter exhibits a strong load dependency. For each normal load in this intermediate range, additional 5-10 independent MD forward-backward friction simulations (total 10 - 15 MD runs) are carried out to calculate the

statistic average of mean friction forces. Figure 2b shows the detailed histogram of the probability of the occurrence of low- and high-friction states under each normal load for the small SiO₂ tip. The figure shows an increasing trend of high-friction states as the normal load is increased. The occurrence of these high-friction states is attributed to the surface defects created at the contact interface, similar to what is shown in **Fig. 3d** for the small SiO₂ tip under $N_{ext} = 18$ nN. In general, the probability of the occurrence of the high-friction state depends on how likely the SiO₂ tip to create surface defects on the Au (111) surface, which is positively related to the applied normal load (Fig. 2b). Approximate potential energy calculations using the empirical potentials employed in this MD simulation study show that the energy difference between the low-friction state (without surface defects) and the high-friction state (with surface defects) is surprisingly low, which is comparable to kT (~25 meV) at room temperature. This energy difference is estimated by freezing the low- and high-friction atomic configurations shown in Fig. 4, which involves the first and second neighboring atoms around the defects, including 12 nearby gold atoms and 1 SiO₄ atomic group. Such a small energy difference indicates that the conformation of the SiO₄ atomic group in contact with the perfect Au (111) surface (Fig. 4a and 4c) is thermodynamically switchable to creating a gold ad-atom on the Au (111) surface, accompanied by a rigid-body rotation of the SiO₄ group to allow the O atom in a Si-O bond to inhabit the gold surface vacancy (Fig. 4b and 4d).

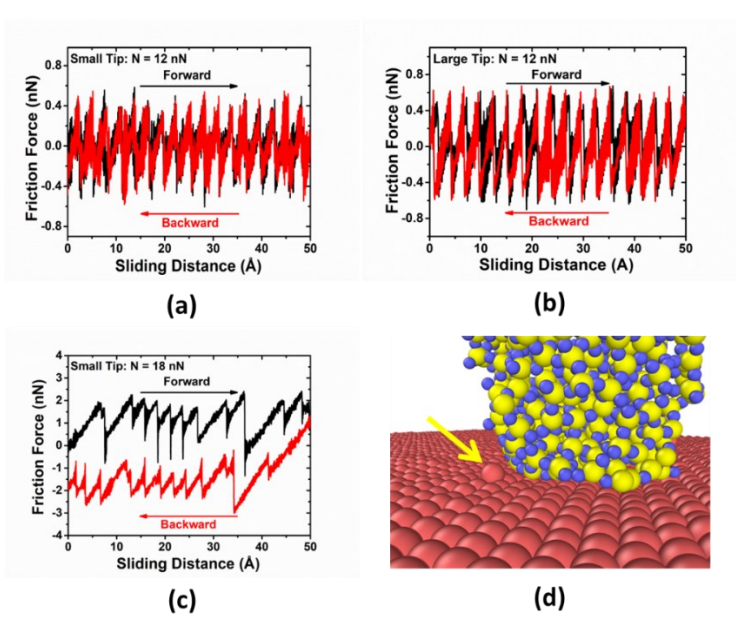


Figure 3. Friction loops of (a) the small tip under 12 nN normal load, (b) the large tip under 12 nN normal load, and (c) the small tip under 18 nN normal load. Panel (d) shows a gold ad-atom (indicated by a yellow arrow) created by the compression of the SiO_2 tip under $N_{ext} = 18$ nN normal load.

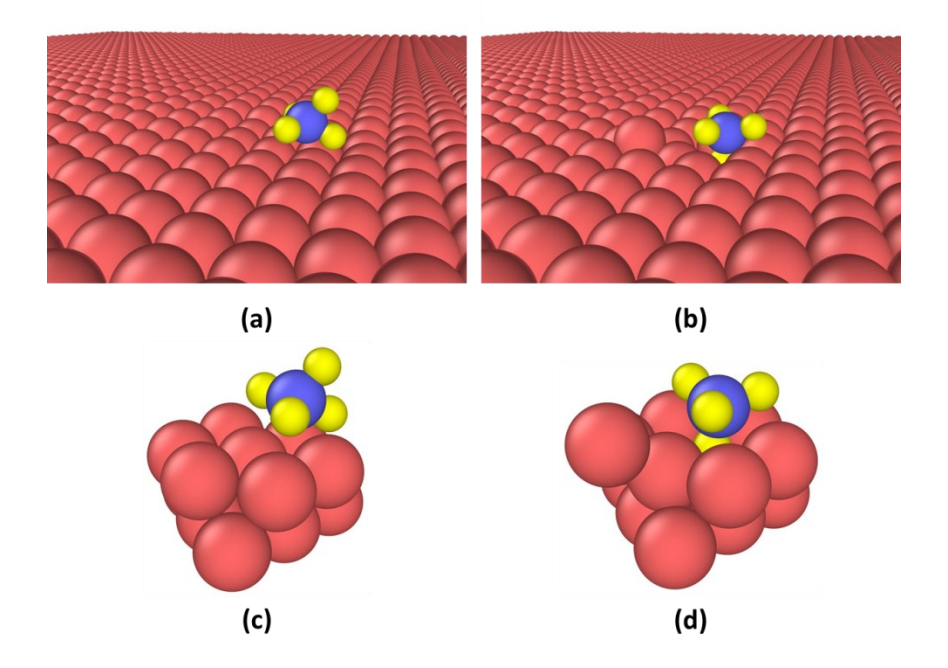


Figure 4. Atomic configurations of (a) the low-friction state without surface defects and (b) the high-friction state with a gold ad-atom on the Au (111) surface, accompanied by a gold surface vacancy occupied by the O atom in a Si-O bond. The normal load is $N_{ext} = 18$ nN. More detailed local atomic configuration changes are shown in (c) and (d). The potential energies associated with the atomic configuration changes in the two states are -74.9432 \pm 0.0602 eV and -74.9682 \pm 0.0637 eV, respectively, giving an energy difference about kT = 25 meV.

Friction duality was first reported when an amorphous Sb nanoparticle was pushed by an AFM tip sliding on a HOPG surface¹⁷. It was found that two distinct friction regimes can coexist, corresponding to a vanishingly low friction due to the incommensurate structural mismatch at the contact interface that led to superlubric friction, and a high friction that is almost linearly dependent of the contact area due to the third-body effect. Here, we find that the friction duality observed in SiO₂/Au (111) contact is linked to the occurrence of surface defects on Au (111) surface. The extremely small energy difference comparable to kT between the non-defect, low-friction state and the high-friction state associated with the plowing friction of a penetrating Si-O bond, can make the two friction scenarios occur under the same normal load.

For the friction simulation of the large SiO₂ tip, except the initial vanishing friction at low loads, we observe a weakly linear dependent friction versus normal load from the intermediate to the high loads (**Fig. 2a**). All simulated friction loops exhibit clear atomic stick-slip friction, similar to that shown in **Fig. 3b**. We find that no surface defects are created during the sliding friction in the full range of normal load investigated (below 45 nN in our simulations). Therefore, no friction

duality is observed. This is certainly because of the actual contact pressure which is much lower than that of the small SiO₂ tip. Moreover, the weakly load-dependent friction of the large SiO₂ tip is similar to that of the small tip in the low-friction state (**Fig. 2a**).

B. How an amorphous SiO₂ tip produces regular stick-slip friction on an Au (111) surface?

The extremely low friction shown in **Fig. 2** when the normal load is below 12 nN is ultimately related to the superlubric behavior due to the structural mismatch between the SiO₂ amorphous tip and the crystalline Au (111) surface. This superlubric behavior is similar to the vanishing friction observed when an amorphous Sb nanoparticle was pushed to slide on a HOPG surface¹⁷. An interesting question concerns how an amorphous SiO₂ tip sliding on an Au (111) surface, even in the superlubric regime, could still produce regular stick-slip friction signals, thus being capable of imaging a crystalline surface? Such stick-slip frictions were observed in experiments ^{10,28}, and are also seen in **Fig. 3a** and **3b** in our simulations.

Here, we take the small SiO₂ tip sliding on the Au (111) surface under $N_{ext} = 12$ nN as an example to further analyze this interesting question. **Figure 5a** shows the more detailed sawtooth-like, stick-slip friction fluctuations during the first 10 Å sliding distance shown in **Fig. 3a**. The lateral displacement of the tip versus the initial 10 Å sliding distance is also shown in the figure, which clearly shows single-slip jumps. Gold atoms jumping to the SiO₂ tip were not observed, in contrast to the case of Pt/Au contact in our previous simulations¹², in which adhesion and fast diffusion of gold atoms result in a large number of Au atoms attached to the Pt tip.

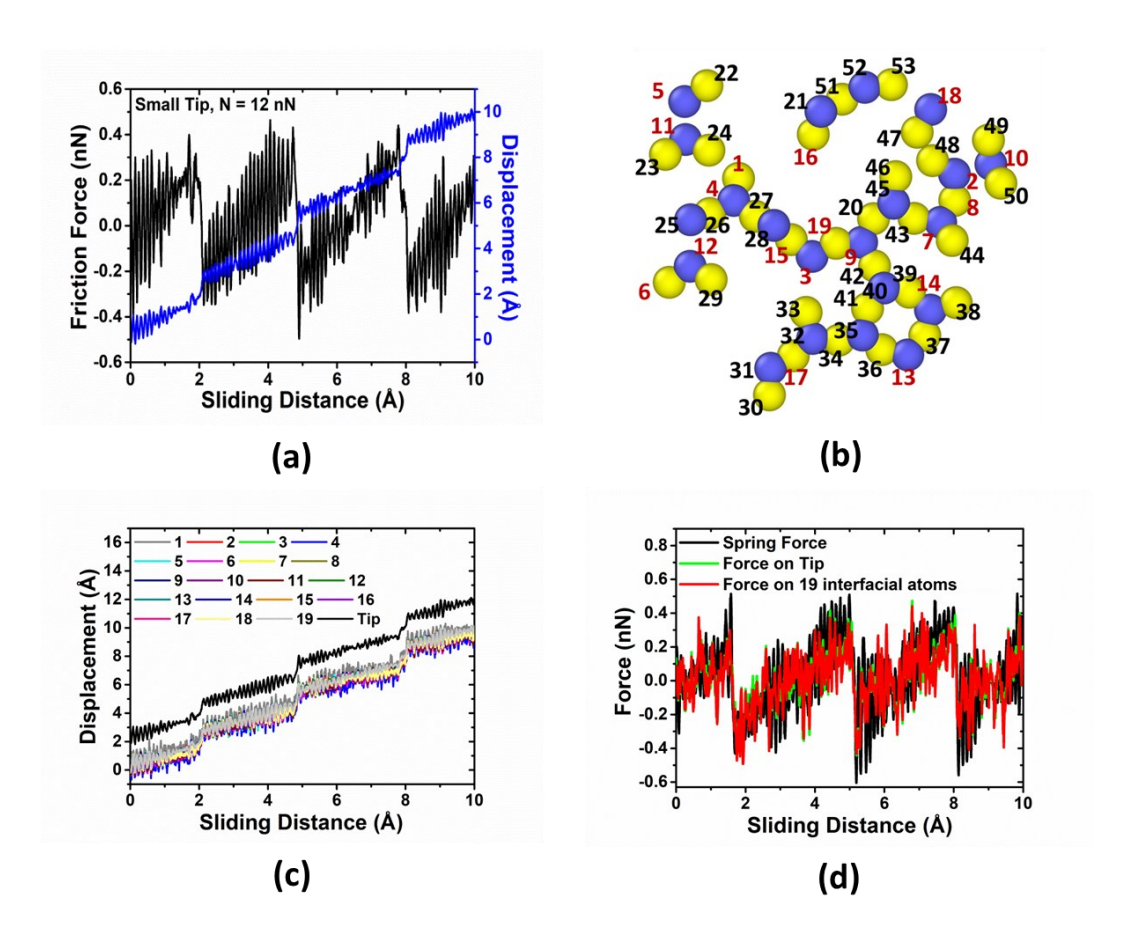


Figure 5. (a) Variations of the stick–slip friction force and actual displacement of the small amorphous SiO_2 tip versus the sliding distance of the driving spring. (b) The 53 atoms in the tip apex with different atom IDs. The 19 contacting atoms are marked in red. (c) The actual displacements of the 19 contacting atoms and the SiO_2 tip. The displacement of the tip is shifted 2A upward for comparison. (d) Comparison of the net lateral force experienced by the 19 contacting atoms with the friction force measured by the spring and the total force experienced by the whole SiO_2 tip. The normal load is $N_{ext} = 12$ nN.

Since stick-slip friction is dominated by the interactions of interfacial atoms at the contact between the SiO₂ tip and the Au (111) substrate, we particularly focus on individual particle forces imposed on the SiO₂ tip apex Si and O atoms from the gold substrate. We therefore carried out the following three detailed analyses. *First*, a total of 53 interfacial Si and O atoms are identified as shown in **Fig. 5b**. These atoms are selected based on their average distance from the gold substrate smaller than 3.3 Å. *Second*, individual normal forces experienced by these Si and O atoms from the gold substrate during the stick-slip sliding are further averaged and sorted, of which a total of 19 atoms (12 Si and 7 O atoms marked in red in **Fig. 5b**) whose average normal forces are greater than 0.2 nN are sorted out. We find that the sum of these individual particle normal forces applied on the 19 atoms nearly accounts for the total normal force experienced by the entire tip. This is shown in **Fig. 6**, indicating that the normal load on the SiO₂ tip is supported only by a small number

of atoms at the contact interface due to the atomic scale roughness on an amorphous surface⁴⁰⁻⁴¹. These forces are then transmitted to the interior region of the tip. *Third*, of the 19 load-bearing atoms, we further calculate individual lateral friction forces on each atom, their net contribution to the total friction force, and atomic displacements of each atom versus sliding distance. The lateral displacements of the 19 contacting atoms and that of the entire SiO₂ tip versus sliding distance are shown in **Fig. 5c**. The displacement of the whole body of the SiO₂ tip is shifted 2 Å upward for comparison. The figure clearly shows that, within thermal fluctuations, all individual atom displacements and the tip displacement overlap during the stick-slip sliding, suggesting that the tip's apex moves coherently as a rigid body.

As shown in **Fig. 5d**, the net lateral friction force experienced by the 19 contacting atoms almost accounts for the friction force measured by the spring and the force experienced by the entire SiO₂ tip. However, these individual atoms can be further divided into three force contribution groups based on the trend of individual atomic force fluctuations relative to the total friction force: (i) in-phase contribution to the total friction force, namely, this group of atoms exhibit friction force fluctuations in concert with the total friction force variations shown in **Fig. 5d**, which include 6 contacting Si and 2 contacting O atoms (**Fig. 7a**); (ii) out-of-phase or inverse contribution to the total friction force. This group of atoms include 3 contacting Si and 1 contacting O atoms whose atomic friction force fluctuations are opposite to the total friction force variations (**Fig. 7b**). Finally, group (iii) atoms include 3 contacting Si and 4 contacting O atoms whose atomic friction forces only exhibit random force fluctuations without any trend with respect to the stick-slip friction (**Fig. 7c**).

Typical snapshots of these three groups of atoms on the Au (111) surface are shown in **Fig. 7d** – **7f**. Group (i) atoms are largely sitting on the relatively stable, close-to-hollow sites of the crystalline Au (111) surface. They are gradually driven away from these relatively stable sites during the stick stage, followed by a sudden slip when jumping over the unstable, close-to-ontop sites of the Au (111) surface. Therefore, this group of atoms are capable of sampling local energy minima. The stick-slip periodic distance corresponds to the Au (111) first neighbor distance of 0.288 nm (see the dashed lines shown in **Fig. 7d**). On the contrary, group (ii) and (iii) atoms largely sit on the metastable, close-to-on-bridge sites (dotted lines), or on the unstable, close-to-ontop sites (dot-dashed lines) of the Au (111) surface, leading to *inverse* stick-slip friction or completely random lateral force fluctuations. Since group (i) atoms always outnumber group (ii) atoms

(otherwise the SiO₂ tip will be very diffusive on the Au (111) surface), a legible stick-slip friction signal can be always seen as shown in **Fig. 5d**. Our consequent conclusion is that in general, it is highly plausible that in AFM friction measurements, one can always use an amorphous silicon tip to image a crystalline metal surface under suitable normal loads. This is even possible in the low-friction state in the intermediate loading range when the friction duality happens.

Our present MD simulation study shows that when an amorphous SiO₂ tip is used to scan a crystalline metal surface, there are always a small fraction of contacting atoms that can effectively image the crystalline atomic structure of the sample surface, producing regular stick-slip friction signals. It is very interesting to see that if we define the contacting atoms as the sorted-out 19 atoms whose average normal forces from the gold substrate are greater than 0.2 nN (Fig. 6), then this fraction number is about 42%. However, if we define the 53 interfacial Si and O atoms whose average distances from the gold substrate are smaller than 3.3 Å as the contacting atoms (Fig. 5b), then this fraction number is further reduced to 15%. These fraction numbers are much smaller than what is seen for a polycrystalline Pt tip scanning an Au (111) surface. From the specific Moiré pattern formed between the bottom layer of the Pt tip and the top layer of the Au (111) substrate, which is shown in Fig. 2 in our previous publication¹², we can easily calculate the actual fraction number of Pt atoms that can effectively image the Au (111) surface is 6/7, or close to 86%. Therefore, it is not surprising that in AFM friction measurements, a crystalline metal tip scanning an Au (111) surface will give a much better stick-slip friction signal than what could be achieved using an amorphous silicon tip, as has been clearly demonstrated in previous experimental studies⁹, 11

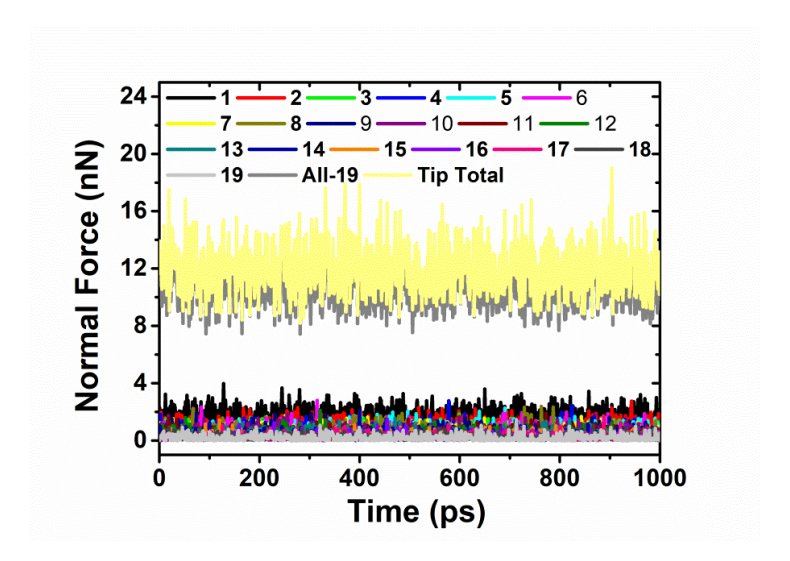


Figure 6. Normal force fluctuations versus time of 1 ns (equivalent to 10 Å sliding distance) associated with the 19 individual contacting atoms. The sum of these 19 individual atomic forces, as well as the total normal force experienced by the entire SiO_2 tip, are also shown for comparison.

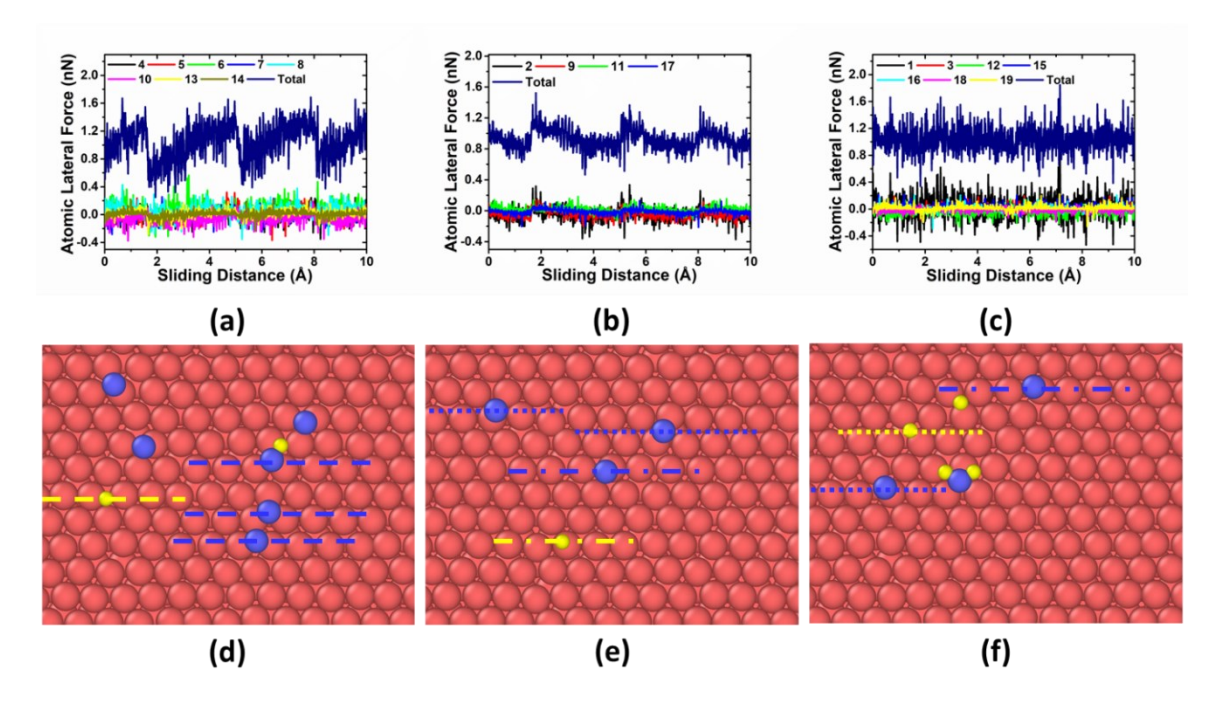


Figure 7. Three friction force contribution groups from the 19 contacting atoms: (a) in-phase contribution to total friction force (against sliding motion); (b) out-of-phase contribution to total friction force (aiding sliding motion), and (c) no clear trend of friction force contribution (random force fluctuations). The total friction force contributed from each group is shifted 1 nN upward for comparison. Panels (d) – (f) show typical snapshots of the three groups of atoms on the Au (111) surface. The normal load is $N_{ext} = 12$ nN.

CONCLUSIONS

The present MD simulation studies of amorphous SiO₂ tips sliding on an Au (111) surface provide the following understandings of the stick—slip friction observed in AFM experiments:

- (1) Negligible friction at low normal loads with clear stick-slip friction signals are observed, similar to what were frequently seen in AFM friction force measurements. The friction is independent of the applied normal load up to 12 nN for both small and large SiO₂ model tips;
- (2) A unique phenomenon of friction *duality* is observed in the intermediate range of applied normal load for the small SiO₂ tip, where friction remains low or increases sharply with the onset of surface defects on the Au (111) surface. The energy difference between the low-friction and high-friction states, where the latter contains a gold ad-atom on the Au (111) and a surface vacancy occupied by an O atom in a Si-O bond, is surprisingly low (comparable to kT at room temperature). The friction duality observed in the present MD simulation study provides a very different interpretation to the high friction found in previous AFM friction measurements, which was attributed to the mechanism of a crystalline metal neck formation between the SiO₂ tip and the Au (111) surface;
- (3) For the large SiO₂ tip sliding on the Au (111) surface, because of the relatively low contact pressures on local contact atoms, only the low-friction state is observed in a very wide range of normal loads, under which no surface defects are seen during stick-slip sliding friction;
- (4) Finally, our MD simulations show that even using an amorphous SiO₂ tip sliding on an Au (111) surface, one can still image a crystalline surface by producing regular stick-slip friction signals. This is largely due to the fact that there are always a small fraction of contacting Si and O atoms at the sliding interface that are capable of sampling local energy minima. These atomic particles are gradually driven away from the relatively stable sites during the stick stage, followed by a sudden slip when jumping over the unstable, close-to-ontop sites of the Au (111) surface. Since the fraction number of imaging atoms in an amorphous SiO₂ tip is much smaller than that of using a crystalline Pt metal tip, the quality of stick-slip friction signals an amorphous silicon tip could provide is inferior to that given by a Pt metal tip, as frequently seen in many AFM friction measurements.

ACKNOWLEDGMENTS

This work is supported by the National Science Foundation (NSF 1953171) and the resources of the National Energy Research Scientific Computing Center (NERSC), a DOE Office of Science User Facility supported by the Office of Science of the U.S. Department of Energy under Contract no. DE-AC02-05CH11231.

REFERENCES

- 1. Vanossi, A.; Manini, N.; Urbakh, M.; Zapperi, S.; Tosatti, E., Colloquium: Modeling Friction: From Nanoscale to Mesoscale. *Reviews of Modern Physics* **2013**, *85*, 529-552.
- 2. Krylov, S. Y.; Frenken, J. W. M., The Physics of Atomic-Scale Friction: Basic Considerations and Open Questions. *Physica Status Solidi B* **2014**, *251*, 711-736.
- 3. Persson, B. N., *Sliding Friction: Physical Principles and Applications*; Springer Science & Business Media, 2013.
- 4. Urbakh, M.; Klafter, J.; Gourdon, D.; Israelachvili, J., The Nonlinear Nature of Friction. *Nature* **2004**, *430*, 525-528.
- 5. Urbakh, M.; Meyer, E., Nanotribology: The Renaissance of Friction. *Nat. Mater.* **2010**, *9*, 8-10.
- 6. Szlufarska, I.; Chandross, M.; Carpick, R. W., Recent Advances in Single-Asperity Nanotribology. *J. Phys. D-Appl. Phys.* **2008**, *41*, 123001.
- 7. Binnig, G.; Quate, C. F.; Gerber, C., Atomic Force Microscope. Phys. Rev. Lett. 1986, 56, 930-933.
- 8. Mate, C. M.; McClelland, G. M.; Erlandsson, R.; Chiang, S., Atomic-Scale Friction of a Tungsten Tip on a Graphite Surface. In *Scanning Tunneling Microscopy*, Springer: 1987; pp 226-229.
- 9. Li, Q. Y.; Dong, Y. L.; Perez, D.; Martini, A.; Carpick, R. W., Speed Dependence of Atomic Stick-Slip Friction in Optimally Matched Experiments and Molecular Dynamics Simulations. *Phys. Rev. Lett.* **2011**, *106*, 126101.
- 10. Gosvami, N. N.; Filleter, T.; Egberts, P.; Bennewitz, R., Microscopic Friction Studies on Metal Surfaces. *Tribol. Lett.* **2010**, *39*, 19-24.
- 11. Liu, X. Z.; Ye, Z. J.; Dong, Y. L.; Egberts, P.; Carpick, R. W.; Martini, A., Dynamics of Atomic Stick-Slip Friction Examined with Atomic Force Microscopy and Atomistic Simulations at Overlapping Speeds. *Phys. Rev. Lett.* **2015**, *114*, 146102.
- 12. Xu, R.-G.; Zhang, G.; Xiang, Y.; Garcia, J.; Leng, Y., Will Polycrystalline Platinum Tip Sliding on a Gold(111) Surface Produce Regular Stick—Slip Friction? *Langmuir* **2022**, *38*, 6808-6816.
- 13. Jacobs, T. D.; Wabiszewski, G. E.; Goodman, A. J.; Carpick, R. W., Characterizing Nanoscale Scanning Probes Using Electron Microscopy: A Novel Fixture and a Practical Guide. *Review of Scientific Instruments* **2016**, *87*, 013703.
- 14. Bennewitz, R., (Personal Communication): 2022.
- 15. Gosvami, N. N.; Feldmann, M.; Peguiron, J.; Moseler, M.; Schirmeisen, A.; Bennewitz, R., Ageing of a Microscopic Sliding Gold Contact at Low Temperatures. *Physical review letters* **2011**, *107*, 144303.
- 16. Petzold, C.; Koch, M.; Bennewitz, R., Friction Force Microscopy of Tribochemistry and Interfacial Ageing for the Siox/Si/Au System. *Beilstein Journal of Nanotechnology* **2018**, *9*, 1647-1658.
- 17. Dietzel, D.; Ritter, C.; Mönninghoff, T.; Fuchs, H.; Schirmeisen, A.; Schwarz, U. D., Frictional Duality Observed During Nanoparticle Sliding. *Phys. Rev. Lett.* **2008**, *101*, 125505.

- 18. Dietzel, D.; Feldmann, M.; Schwarz, U. D.; Fuchs, H.; Schirmeisen, A., Scaling Laws of Structural Lubricity. *Physical review letters* **2013**, *111*, 235502.
- 19. Dietzel, D.; Schwarz, U. D.; Schirmeisen, A., Nanotribological Studies Using Nanoparticle Manipulation: Principles and Application to Structural Lubricity. *Friction* **2014**, *2*, 114-139.
- 20. Carpick, R. W.; Ogletree, D. F.; Salmeron, M., A General Equation for Fitting Contact Area and Friction Vs Load Measurements. *Journal of colloid and interface science* **1999**, *211*, 395-400.
- 21. Dong, Y.; Li, Q.; Martini, A., Molecular Dynamics Simulation of Atomic Friction: A Review and Guide. *Journal of Vacuum Science & Technology A: Vacuum, Surfaces, and Films* **2013**, *31*, 030801.
- 22. Mo, Y.; Turner, K. T.; Szlufarska, I., Friction Laws at the Nanoscale. *Nature* **2009**, *457*, 1116-1119.
- 23. Pietrement, O.; Troyon, M., Study of the Interfacial Shear Strength Pressure Dependence by Modulated Lateral Force Microscopy. *Langmuir* **2001**, *17*, 6540-6546.
- 24. Gao, J.; Luedtke, W.; Gourdon, D.; Ruths, M.; Israelachvili, J.; Landman, U., Frictional Forces and Amontons' Law: From the Molecular to the Macroscopic Scale. ACS Publications: 2004; Vol. 108, pp 3410-3425.
- 25. Luan, B.; Robbins, M. O., The Breakdown of Continuum Models for Mechanical Contacts. *Nature* **2005**, *435*, 929-932.
- 26. Schwarz, U. D.; Zwörner, O.; Köster, P.; Wiesendanger, R., Quantitative Analysis of the Frictional Properties of Solid Materials at Low Loads. I. Carbon Compounds. *Physical Review B* **1997**, *56*, 6987.
- 27. Wenning, L.; Müser, M., Friction Laws for Elastic Nanoscale Contacts. *EPL (Europhysics Letters)* **2001**, *54*, 693.
- 28. Bennewitz, R.; Hausen, F.; Gosvami, N. N., Nanotribology of Clean and Modified Gold Surfaces. *J. Mater. Res.* **2013**, *28*, 1279-1288.
- 29. Landman, U.; Luedtke, W.; Burnham, N. A.; Colton, R. J., Atomistic Mechanisms and Dynamics of Adhesion, Nanoindentation, and Fracture. *Science* **1990**, *248*, 454-461.
- 30. So, M.; Jacobsen, K. W.; Stoltze, P., Simulations of Atomic-Scale Sliding Friction. *Physical Review B* **1996**, *53*, 2101.
- 31. Merkle, A. P.; Marks, L. D., Liquid-Like Tribology of Gold Studied by in Situ Tem. *Wear* **2008**, *265*, 1864-1869.
- 32. Daw, M. S.; Baskes, M. I., Semiempirical, Quantum Mechanical Calculation of Hydrogen Embrittlement in Metals. *Physical review letters* **1983**, *50*, 1285.
- 33. Foiles, S.; Baskes, M.; Daw, M. S., Embedded-Atom-Method Functions for the Fcc Metals Cu, Ag, Au, Ni, Pd, Pt, and Their Alloys. *Physical review B* **1986**, *33*, 7983.
- 34. Voter, A. F., Embedded Atom Method Potentials for Seven Fcc Metals: Ni, Pd, Pt, Cu, Ag, Au, and Al. *Los Alamos Unclassified Technical Report# LA-UR* **1993**, 93-3901.
- 35. Tersoff, J., Empirical Interatomic Potential for Silicon with Improved Elastic Properties. *Physical Review B* **1988**, *38*, 9902.
- 36. Plimpton, S., Fast Parallel Algorithms for Short-Range Molecular Dynamics. *Journal of computational physics* **1995**, *117*, 1-19.
- 37. Thompson, A. P., et al., Lammps a Flexible Simulation Tool for Particle-Based Materials Modeling at the Atomic, Meso, and Continuum Scales. *Computer Physics Communications* **2022**, *271*, 108171.
- 38. Nosé, S., A Unified Formulation of the Constant Temperature Molecular Dynamics Methods. *The Journal of chemical physics* **1984**, *81*, 511-519.
- 39. Hoover, W. G., Canonical Dynamics: Equilibrium Phase-Space Distributions. *Physical review A* **1985**, *31*, 1695.
- 40. Cheng, S.; Robbins, M. O., Defining Contact at the Atomic Scale. *Tribol. Lett.* **2010**, *39*, 329-348.
- 41. Wang, Y.; Qin, J.; Xu, J.; Sun, J.; Chen, L.; Qian, L.; Kubo, M., Definition of Atomic-Scale Contact: What Dominates the Atomic-Scale Friction Behaviors? *Langmuir* **2022**, *38*, 11699-11706.

TOC Graphic

